A hybrid approach to Simulate X-ray imaging techniques, combining Monte Carlo and deterministic algorithms

Article *in* IEEE Transactions on Nuclear Science · November 2005

DOI: 10.1109/TNS.2005.858223 · Source: IEEE Xplore

Jm Létang
Creatis Medical Imaging Research Center

A Hybrid Approach to Simulate X-Ray Imaging Techniques, Combining Monte Carlo and Deterministic Algorithms

Nicolas Freud, Jean-Michel Létang, and Daniel Babot

Abstract— **In this paper, we propose a hybrid approach to simulate multiple scattering of photons in objects under X-ray inspection, without recourse to parallel computing and without any approximation sacrificing accuracy. Photon scattering is considered from two points of view: it contributes to X-ray imaging and to the dose absorbed by the patient. The proposed hybrid approach consists of a Monte Carlo stage followed by a deterministic phase, thus taking advantage of the complementarity between these two methods. In the first stage, a set of scattering events occurring in the inspected object is determined by means of classical Monte Carlo simulation. Then this set of scattering events is used to compute the energy imparted to the detector, with a deterministic algorithm based on a "forced detection" scheme. As regards dose evaluation, we propose to assess separately the energy deposited by direct radiation (using a deterministic algorithm) and by scattered radiation (using our hybrid approach). The results obtained in a test case are compared to those obtained with the Monte Carlo method alone (Geant4 code) and found to be in excellent agreement. The proposed hybrid approach makes it possible to simulate the contribution of each type (Compton or Rayleigh) and order of scattering, separately or together, with a single PC, within reasonable computation times (from minutes to hours, depending on the required detector resolution and statistics). It is possible to simulate radiographic images virtually free from photon noise. In the case of dose evaluation, the hybrid approach appears particularly suitable to calculate the dose absorbed by regions of interest (rather than the entire irradiated organ) with computation time and statistical fluctuations considerably reduced in comparison with conventional Monte Carlo simulation.**

Index Terms— **Rayleigh and Compton scattering, X-ray imaging, Monte Carlo method, deterministic simulation, hybrid simulation, forced detection, dose calculation.**

I. INTRODUCTION

DURING the last decade, several research groups have investigated the issue of fast simulation of X-ray imaging. It is now well established that deterministic algorithms based on ray tracing techniques make it possible to simulate in a short time realistic radiographs, taking into account polychromatic X-rays, intricate three-dimensional objects, geometric unsharpness, etc. [1]–[3]. Actually, the deterministic approach proves really fast at the expense of physical accuracy: only direct radiation (i.e. photons that do not interact in the object before being detected) is usually considered. To assess the role of scattered radiation (and, possibly, of secondary radiation), several groups have proposed quite sophisticated methods, based on deterministic or stochastic approaches [4]–[8]. The computing resources required by these approaches are considerable, and parallel implementations have been reported [9], [10].

In this context, we have recently proposed a hybrid simulation approach, combining Monte Carlo and deterministic algorithms, to simulate multiple photon scattering [11]. This work has demonstrated the feasibility of simulating the contribution of multiple scattering to transmission images, with limited computing resources (single PC).

In the present paper, we address the simulation of multiple scattering from two viewpoints: transmission imaging and dose deposition in the irradiated sample. As a test case, we will consider a polymethyl methacrylate (PMMA) step wedge irradiated with 20 keV X-rays.

The outline of this paper is as follows: after summarizing the principle of the hybrid approach, we illustrate its performance with an example in the case of transmission imaging; then we broach the calculation of the dose deposited in the sample by direct and scattered radiation. We compare our results to those obtained with the Monte Carlo method alone (Geant4 code) in the same configuration.

II. PRINCIPLE OF THE METHOD

The proposed hybrid method consists of two stages (Fig. 1):

- Firstly, a set of scattering events occurring in the inspected object is determined by means of classical Monte Carlo simulation. Each photon is tracked from its point of emission to the point where it is absorbed or crosses the boundaries of the simulated experiment. Each time the photon is scattered, the coordinates of the interaction point, the direction of propagation and the energy of the incident photon, as well as the type (Rayleigh or Compton) and order of scattering are recorded.
- Secondly, the set of scattering events is used to compute the energy imparted to the detector, with a deterministic algorithm based on a "forced detection" scheme [12], [13].

In both the Monte Carlo and deterministic stages, the same physical models are used, namely the form factor (FF) and the incoherent scattering function (ISF) approximations,

N. Freud, Jean-Michel Létang, and Daniel Babot are with the Laboratory of Nondestructive Testing using Ionizing Radiations, INSA-Lyon Scientific and Technical University, Bât. Antoine de Saint-Exupéry, 20, avenue Albert Einstein, 69621 Villeurbanne Cedex, France (e-mail of corresponding author: Nicolas.Freud@insa-lyon.fr).

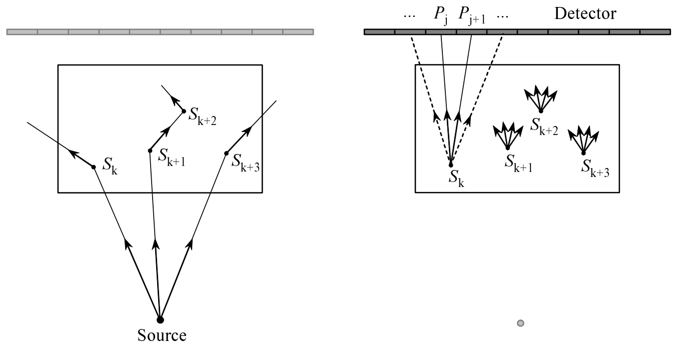

Fig. 1. The hybrid simulation method consists of two stages. The first stage is a Monte Carlo simulation, whose result is a list of scattering events $\{S_1,\ldots,S_k,S_{k+1},\ldots,S_n\}$ (left). This list is used during the second stage, in which scattering is forced towards every pixel of the detector (right).

for Rayleigh and Compton scattering of unpolarized photons respectively. The FF and ISF values, as well as the mass attenuation coefficients are taken from the EPDL97 database, distributed by Cullen et al. [14].

A. Case of imaging: detector placed outside the sample

For each scattering point S_k, the probability for the scattered photon to reach pixel P_j of the detector is given by

$$\mathrm{d}p_{kj} = \frac{1}{\sigma_k(E_k^i)} \frac{\mathrm{d}\sigma_{kj}(\theta_{kj}, E_k^i)}{\mathrm{d}\Omega_{kj}} \exp\left[-\mu(E_{kj}^s) x_{kj}\right] \mathrm{d}\Omega_{kj}, \quad (1)$$

where $\sigma_k(E_k^i)$ is the total cross section for scattering off S_k over 4π sr, function of the energy E_k^i of the incident photon, $\mathrm{d}\sigma_{kj}/\mathrm{d}\Omega_{kj}$ is the differential cross section (DCS), function of the scattering angle θ_{kj} and of E_k^i, μ is the linear attenuation coefficient, function of the energy E_{kj}^s of the scattered photon, x_{kj} is the attenuation path length traversed by the scattered ray in the object and $\mathrm{d}\Omega_{kj}$ is the solid angle corresponding to pixel P_j seen from scattering point S_k. The probability $\mathrm{d}p_{kj}$ given by (1) has to be computed for each scattering event in the object and for each pixel of the detector. This calculation is completely deterministic. Assuming the detector to be perfect (i.e. that is detects all the photons that hit its surface and integrates their energy), the final image is obtained by summing the contributions of all scattering points S_k. The energy received by pixel P_j is given by

$$E_j = \sum_k \mathrm{d}p_{kj} E_{kj}^s. \quad (2)$$

B. Case of dosimetry: detector placed inside the sample

To compute dose profiles or maps, we place a virtual detector inside the irradiated sample. The dose deposited at voxel V_j by photons coming from S_k is given by

$$D_j = E_{kj}^s \Phi_{kj}^s \, \mu_d(E_{kj}^s)/\rho \quad (3)$$

where Φ_{kj}^s is the photon fluence scattered off S_k towards V_j and μ_d/ρ is the mass energy-deposition coefficient, function of energy. The photon fluence, defined as the number of photons per unit area, satisfies

$$\Phi_{kj}^s = \frac{1}{r_{kj}^2} \frac{\mathrm{d}p_{kj}}{\mathrm{d}\Omega_{kj}}, \quad (4)$$

where r_{kj} is the distance from scattering point S_k to the center of voxel V_j.

In this work, the energy lost by photons during photoelectric or Compton events is assumed to be deposited locally. Three arguments back up this assumption:

- The range of electrons is much smaller than the scale of observation. In the test case chosen for this paper, the range of electrons in PMMA, at 20 keV, is about 7 μm (range calculated in the continuous-slowing-down approximation), whereas the voxel size is 1 mm. More generally, electrons with a kinetic energy below 100 keV have a range in soft tissue shorter than 150 μm [15].
- The radiation yield (average fraction of the initial kinetic energy of an electron that is converted to bremsstrahlung energy) is very low, in the energy range of diagnostic X-rays. In other words, there is very little energy escaping as bremsstrahlung emission during the slowing down of electrons, because collisional energy losses are by far the dominating process. For example, in PMMA, the radiation yield is smaller than 10^{-3} for electrons with kinetic energy below 200 keV [15].
- In low-Z elements ($Z < 10$), all radiative transitions are below 1 keV, therefore a very short distance (a few micrometers in our test case) is sufficient for all fluorescence photons to be absorbed. Note, however, that in materials containing higher-Z elements, higher-energy fluorescence photons would travel longer distances and, therefore, would have to be taken into account in the simulation.

Finally, $\mu_d(E)/\rho$ can be written as

$$\frac{\mu_d(E)}{\rho} = \frac{\mu_{\mathrm{ph}}(E)}{\rho} + \frac{\mu_{\mathrm{Co}}(E)}{\rho} \; \frac{E - \langle E_{\mathrm{Co}} \rangle}{E}, \quad (5)$$

where μ_{ph}/ρ and μ_{Co}/ρ are the mass attenuation coefficients for photoelectric and Compton effects respectively, and $\langle E_{\mathrm{Co}} \rangle$ is the average energy of the Compton-scattered photon (also function of the incident photon energy). All these data are available in EPDL97 [14].

III. Results in a test case and comparison with the Monte Carlo method

A. Simulated configuration

We have chosen to test our hybrid method in the configuration presented in Fig. 2. The first simulation stage was carried out with the Monte Carlo code Geant4 (release 6.0, patch 01) [16]. The incident photons were generated with equiprobable directions within a cone beam. Only photons were tracked in the simulation (electronic processes were inactivated). The spatial distribution of the scattering interactions in the sample can be visualized in Fig. 3.

To illustrate the highly anisotropic character of Rayleigh and Compton interactions, we have represented their DCSs, in the FF and ISF approximations respectively, in the case of PMMA, at 20 keV (Fig. 4).

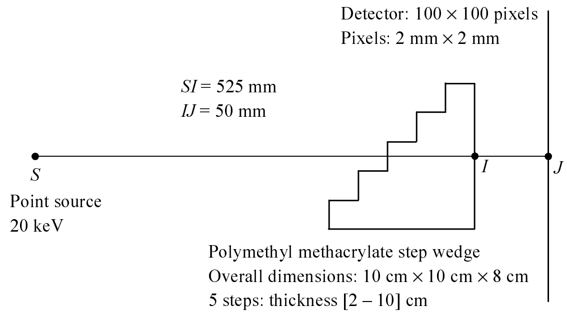

Fig. 2. Geometric arrangement of the simulated experiment. The incident photons are emitted isotropically in a cone with half angle at the apex $\theta_{\max} = 0.242$ rad. A radiographic image is obtained on the detector placed behind the step wedge (this detector is considered to be perfect). Besides the radiographic image, a dose map is computed in the vertical symmetry plane (100×100 cubic voxels of 1 mm^3).

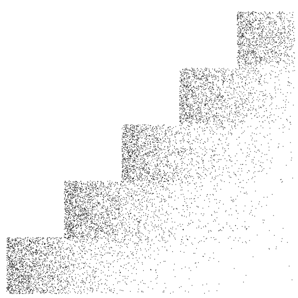

Fig. 3. Orthographic projection of 10^4 scattering events (about 7.1×10^3 Compton and 2.9×10^3 Rayleigh events) generated by the Monte Carlo stage in the configuration of Fig. 2.

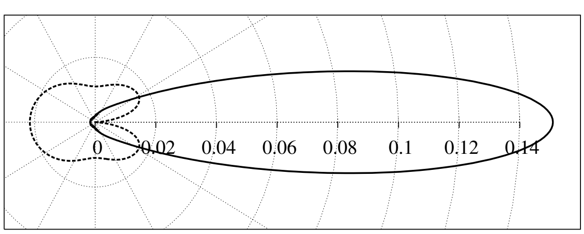

Fig. 4. DCSs for Rayleigh (solid line) and Compton (dashed line) scattering of unpolarized radiation in PMMA, in $\mathrm{cm}^2 \cdot \mathrm{g}^{-1} \cdot \mathrm{sr}^{-1}$, computed using the FF and ISF values tabulated in EPDL97.

B. Role of multiple scattering in transmission imaging

We have simulated the image formed by scattered radiation with our hybrid approach, with 5×10^5 incident photons, which generated 55640 scattering points in the first simulation stage; all these scattering events were processed in the second stage. The whole simulation took 10 minutes with a 2.8 GHz processor (PC architecture). To validate our hybrid simulation method and to assess its performance, we have simulated the same experiment (except for the number of incident photons, which was set to 5×10^8) with the Monte Carlo method alone (Geant4 code). This simulation took about 20 hours. The results of both approaches are presented in Fig. 5, and the profiles extracted from the 50th (central) detector column in Fig. 6. Remarkably, the results of the hybrid approach are very smooth, compared to the Monte Carlo simulation, even though the latter involved many more incident photons. Apart from noise, the agreement between the two methods is excellent.

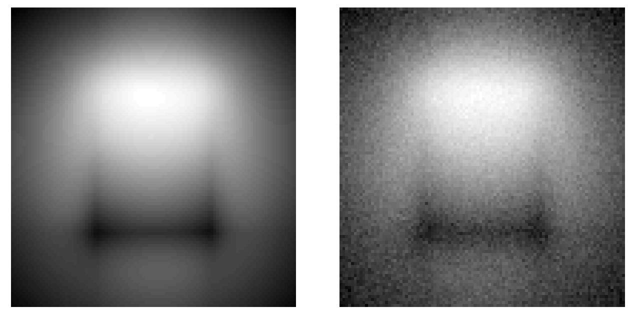

Fig. 5. Simulated image formed by scattered radiation, obtained with the hybrid approach, with 5×10^5 incident photons (left) and with the Monte Carlo approach, using 5×10^8 incident photons (right). Computation times were about 10 min (hybrid) and 20 h (Geant4), with a 2.8 GHz processor (PC architecture).

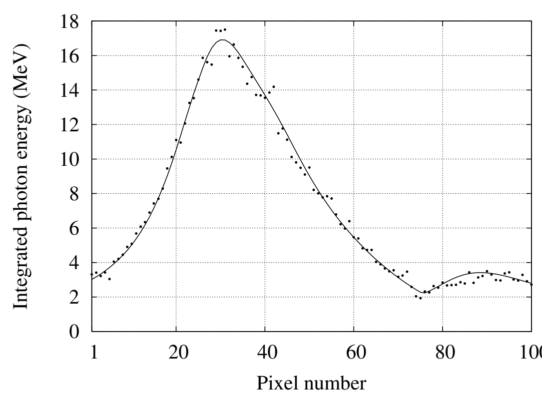

Fig. 6. Profiles corresponding to the 50th column of the images of Fig. 5 (hybrid simulation: solid line; Monte Carlo simulation: dots). The results of the hybrid method were multiplied by 10^3 to correspond to the same number of incident photons (5×10^8) as in the Monte Carlo simulation.

C. Dose deposited by direct radiation

The dose deposited in the sample at V_j by the radiation coming directly from the X- or γ-ray source can be computed using a simplified version of (3):

$$D_j = E^i \Phi_j^i \, \mu_d(E^i)/\rho, \tag{6}$$

where E^i is the incident photon energy and Φ_j^i the incident photon fluence at V_j. If the source emits a polychromatic spectrum, the calculation has to be repeated for a set of energy values and the corresponding doses are summed. Even with a polychromatic spectrum and a complex geometric configuration, the computation can be carried out in a very short time (typically a few seconds) using a fully deterministic algorithm. It is worthy of note that (6) gives the expectation of the absorbed dose, without any statistical fluctuation. The results obtained in our test case are presented in Fig. 7. Profiles extracted from the images are plotted in Fig. 8. Note that we have chosen to present our results in terms of deposited energy (MeV per voxel), rather than in grays. The agreement between the results of the deterministic and Monte Carlo methods is excellent. In contrast to the Monte Carlo results, the deterministic method gives an image free of noise.

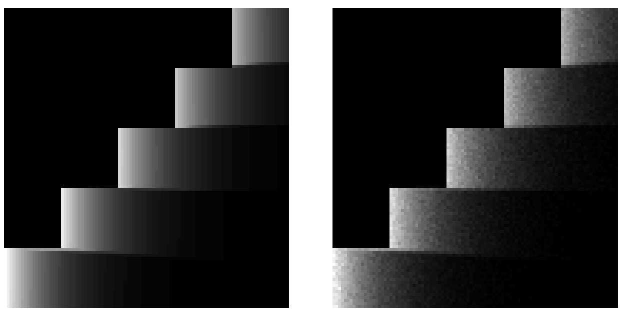

Fig. 7. Energy deposited by direct radiation (5×10^8 incident photons), obtained with the deterministic approach (left) and compared with the results of the Monte Carlo method (right). Computation times were about 1 s (deterministic) and 20 h (Geant4), with a 2.8 GHz processor (PC architecture).

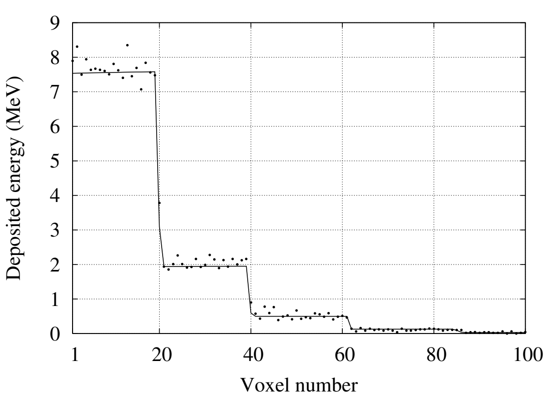

Fig. 8. Profiles corresponding to the 82th column of the images of Fig. 7 (deterministic approach: solid line; Geant4: dots).

D. Dose deposited by scattered radiation

Keeping the same test case, we have computed maps of the dose deposited by scattered radiation, using the hybrid approach. We have carried out simulations with increasing numbers of incident photons to test the convergence of our results. Two dose maps are presented in Fig. 9, and profiles taken at the 82th column of the detector are plotted in Fig. 10.

The bright dots in the images (or peaks in the profiles) are

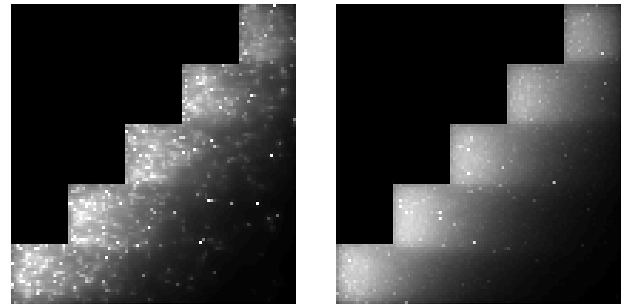

Fig. 9. Energy deposited by scattered radiation, computed using the proposed hybrid approach. The first image (left) was obtained by processing 5×10^4 scattering points (corresponding to about 5×10^5 incident photons). The second image (right) was obtained with 5×10^6 scattering points (about 5×10^7 incident photons). Simulations carried out in about 10 min and 16 h respectively (2.8 GHz processor, PC architecture).

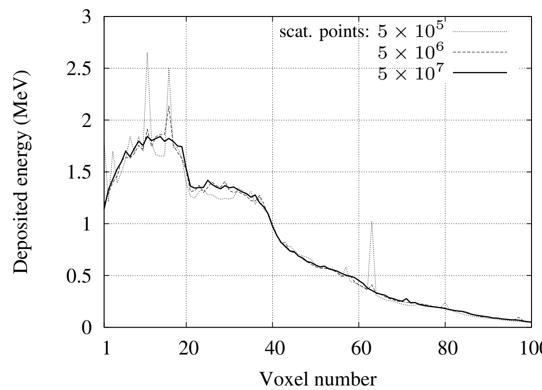

Fig. 10. Profiles corresponding to the 82th column of the detector, obtained with the hybrid approach, with increasing numbers of scattering points, and scaled up to correspond to 5×10^8 incident photons. The first simulation (5×10^5 scattering points) took about 25 min, with nearly equal times spent in the two simulation stages. The two other simulations lasted 10 and 100 times longer.

the signature of scattering points located within short distance of the voxel array. As the photon fluence Φ^s_{kj} scattered off S_k towards V_j is proportional to $1/r^2_{kj}$, the scattering points that happen to be near voxel centers are the source of very high dose contributions for these voxels. This type of artifact is a consequence of voxel discretization (Φ^s_{kj} is computed at the center of voxel V_j) combined with insufficient statistics. Globally, as the number of scattering points processed in the simulation increases, the results become smoother and smoother (see Fig. 9). The profiles, once scaled up to correspond to the same number of incident photons, converge. Finally, the excellent agreement between the hybrid and Monte Carlo methods is illustrated in Fig. 11 and 12.

The performance of the hybrid approach gives rise to the following comments:

- The computation time spent in the deterministic stage is roughly proportional to the number of voxels in the volume of interest. Therefore the hybrid approach is particularly suitable to compute dose maps limited to regions of interest or profiles, rather than 3D dose distributions.

- For a given number of incident photons, the hybrid approach makes it possible to improve considerably the results given by conventional Monte Carlo simulations, by reducing statistical fluctuations.

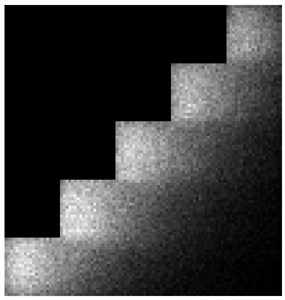

Fig. 11. Energy deposited by scattered radiation, computed using Geant4, with 5×10^8 incident photons.

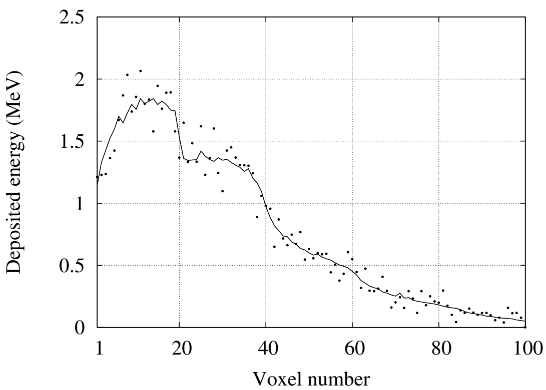

Fig. 12. Profiles corresponding to the 82th column of the detector, obtained with the hybrid approach (solid line) and with Geant4 (dots). The same number of incident photons (5×10^8) was used in both simulations.

IV. Conclusion and perspectives

This work demonstrates that the proposed hybrid simulation method is efficient to simulate the contribution of scattered radiation to X- or γ-ray images and to the dose deposited in the irradiated sample. Evidently, the hybrid approach is also particularly suitable to simulate techniques for which scattered radiation (or secondary radiation) represents the signal of interest. This approach constitutes an alternative to conventional methods (probabilistic or deterministic), which opens up new possibilities.

In this work, we did not try to optimize our simulation code from the point of view of computation time, to focus on the properties of the hybrid method in itself. However, it should be kept in mind that well-known variance reduction techniques, such as Russian roulette and splitting may be used to further improve the performance of the hybrid approach. For example, Russian roulette can be used to kill scattering points located far from the detector (the contribution of such points to the image or dose map is very limited).

In a short term perspective, further work is needed to limit the artifacts due to scattering points located within short distance of the detector. We consider using splitting or a strategy of spatial averaging. We also plan to extend the scope of the hybrid approach by addressing the simulation of fluorescence and bremsstrahlung emission.

References

[1] F. Inanc, J. N. Gray, T. Jensen, and J. Xu, "Human body radiography simulations: development of a virtual radiography environment," in *Physics of Medical Imaging*, vol. 3336. San Diego, California: SPIE – The International Society for Optical Engineering, February 1998, pp. 830–837.

[2] D. Lazos, Z. Kolitsi, and N. Pallikarakis, "A software data generator for radiographic imaging investigations," *IEEE Trans. Inform. Technol. Biomed.*, vol. 4, no. 1, pp. 76–79, 2000.

[3] P. Duvauchelle, N. Freud, V. Kaftandjian, and D. Babot, "A computer code to simulate X-ray imaging techniques," *Nucl. Instrum. Methods B*, no. 170, pp. 245–258, 2000.

[4] F. Inanc and J. N. Gray, "Scattering simulations in radiography," *Applied Radiations and Isotopes*, vol. 48, no. 10–12, pp. 1299–1305, 1997.

[5] F. Inanc, "Scattering and its role in radiography simulations," *NDT&E International*, vol. 35, pp. 581–593, 2002.

[6] G.-R. Tillack, C. Bellon, V. M. Artemiev, and A. O. Naumov, "Simulation of scattering process in radiation techniques exploiting the theory of Markovian processes with random structure," in *Review of Progress in Quantitative Nondestructive Evaluation*, D. O. Thompson and D. E. Chimenti, Eds., vol. 16. New York: Plenum Press, 1997, pp. 309–316.

[7] D. Lazos, K. Bliznakova, Z. Kolitsi, and N. Pallikarakis, "An integrated research tool for x-ray imaging simulation," *Computer Methods and Programs in Biomedicine*, vol. 70, pp. 241–251, 2003.

[8] N. Freud, P. Duvauchelle, S. A. Pistrui-Maximean, J.-M. Létang, and D. Babot, "Deterministic simulation of first-order scattering in virtual x-ray imaging," *Nucl. Instrum. Methods B*, no. 222, pp. 285–300, 2004.

[9] J. Giersch, A. Weidemann, and G. Anton, "ROSI—an object-oriented and parallel-computing Monte-Carlo simulation for X-ray imaging," *Nucl. Instrum. Methods A*, vol. 509, pp. 151–156, 2003.

[10] F. Inanc, B. Vasiliu, and D. Turner, "Parallel implementation of the integral transport equation-based radiography simulation code," *Nuclear Science and Engineering*, vol. 137, pp. 173–182, 2001.

[11] N. Freud, J.-M. Létang, and D. Babot, "A hybrid approach to simulate multiple photon scattering in x-ray imaging," *Nucl. Instrum. Methods B*, accepted for publication.

[12] J. W. Beck, R. J. Jaszczak, R. E. Coleman, C. F. Starmer, and L. W. Nolte, "Analysis of SPECT including scatter and attenuation using sophisticated Monte Carlo modeling methods," *IEEE Trans. Nucl. Sci.*, vol. 29, no. 1, pp. 506–511, 1982.

[13] D. R. Haynor, *Monte Carlo calculations in nuclear medicine*, ser. Medical Science Series. Bristol and Philadelphia: Institute of Physics, 1998, ch. 2, pp. 13–24.

[14] D. E. Cullen, J. H. Hubbell, and L. Kissel, "EPDL97: the evaluated photon data library, '97 version," Lawrence Livermore National Laboratory, Tech. Rep. UCRL–ID–50400, Vol. 6, Rev. 5, September 1997, 36 p.

[15] M. J. Berger, J. S. Coursey, and M. A. Zucker, "Stopping-power and range tables for electrons, protons, and helium ions," [Online], April 2000 (last update), available: http://physics.nist.gov/PhysRefData/Star/Text/contents.html.

[16] S. Agostinelli, J. Allison, K. Amako, J. Apostolakis, H. Araujo, P. Arce, et al. "Geant4—a simulation toolkit," *Nucl. Instrum. Methods A*, no. 506, pp. 250–303, 2003.